J Electr Eng Technol.2018; 13(6): 2292-2300
http://doi.org/10.5370/JEET.2018.13.6.2292

ISSN(Print) 1975-0102
ISSN(Online) 2093-7423

Analysis and Correction of Through-bolt End-region Overheating and Breakdown Failure in a Large Tubular Hydro-generator

Zhi-ting Zhou*, Zhen-nan Fan†, Jian-fu Li, Kun Wen*, Bide Zhang*, Tao Wang*, Yan-kun Xia*, Zhang Sun* and Bing Yao***

Abstract – A field-circuit coupling model of a typical faulty generator is established to correct through-bolt end-region overheating and breakdown failure in a tubular hydro-generator. Using the model, eddy current loss and electromagnetic forces on through bolts under normal and failure conditions are analyzed and compared and the natural frequency of a through bolt is determined. Based on the analysis results, the causative mechanism of failure is revealed and targeted improvement design measures are proposed. The numerical results are found to be consistent with the actual fault characteristics, validating the design measure improvements. The results are useful in improving the design and manufacturing standards and enhancing the operational reliability of large tubular hydro-generators.

Keywords: Failure analysis, Hydroelectric generators, Eddy currents, Electromagnetic forces.

1. Introduction

As a good type of generator for the development of lower head and large flow of water resources, tubular hydro-generators are widely used and continue to be constructed throughout China. However, in recent years, there have been occurrences of stator through-bolt end-region overheating and breakdown faults in several large tubular hydro-generators; these events have even posed danger to the operational security of the generator in some cases.

On-site investigations have revealed several common characteristics for such failures. First, all damaged through bolts were located beneath core bars, and in all cases, the damage was located in the end-region of the bolt. Second, the bolts end-regions had a considerable buildup of greasy dirt. Third, some of the core bars demonstrated overheating traces. Fourth, some of the damaged bolts demonstrated, in addition to signs of overheating and melting, transverse fatigue fracture characteristics. Fifth, the insulation resistance of damaged through bolts to the ground was found to be zero. Some of the failure characteristics listed above are shown in Fig. 1.

Unfortunately, as of now, there are few public literature literature reports on the analysis and resolution of such new failures. However, simultaneously and fortunately, physical field analysis methods have been widely applied in generator performance analysis in recent years. Therefore, it is possible to provide some useful reference for us to analyze this kind of failure [1-18]. For example, [1] and [2] used a permeance model with the Fourier expansion approach to predict the damper bar currents. An analytical algorithm based on equivalent network was adopted in [3] to analyze the damper bar currents and losses when the generator is operated at the rated and the no-load conditions. Furthermore, [4] proposed a combined numerical and analytical method for the computation of unbalanced magnetic pulls, damper bar currents, and losses of laminated low speed hydro-generators in eccentricity conditions under no-load. Studies [5, 6], and [7] considered the effect of rotor rotation when analyzing generator performance. To consider the influence of end windings and load conditions more fully, [8-14], and [15] used the field-circuit coupling model in the electric machinery performance analysis. Among these, [11-13], and [14] analyzed the performance of the slot skewed electric machinery, whereas [13, 14], and [15] analyzed and solved the eddy current and loss of damper bars of the hydro generator. In addition, [16, 17], and [18] analyzed and solved the heating problem of the hydro generator by establishing a model of the fluid field and temperature field.

In this study, the occurrence mechanisms of through-bolt end-region failure were determined through field-circuit coupling and modal analysis. The results were then used to provide the proposed design measure improvements to successfully eliminate the failure.

† Corresponding Author: The Key Laboratory of Fluid and Power Machinery, Ministry of Education, Xihua University, Chengdu China. (fanzhennan@126.com)
* The Key Laboratory of Fluid and Power Machinery, Ministry of Education, Xihua University, Chengdu, China. ({dianyingcc, wkk_xhu, kk_xhu, chengbg_a, yaob_xhu}@126.com, {43357942, 383623076}@qq.com,xy)
** Dong Fang Electrical Machinery Co., Ltd., Deyang, China. (zouhui_a@126.com)
Received: January 1, 2018; Accepted: June 23, 2018

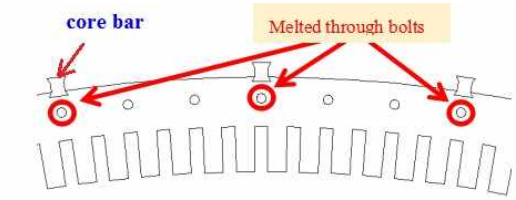

(a) All damaged bolts are below core bars

(b) Through-bolt end-region overheating, melting, and breakdown

(c) Through-bolt end-region overheating and melting along with transverse fatigue fracturing

(d) Core bar overheating, with damaged bolt end-region showing significant greasy dirt buildup

Fig. 1. Failure characteristics

2. Field-circuit Coupling Calculation Models

2.1 Potential failure mechanism and basic generator data

The failure characteristics listed above, in particular, the key features of zero insulation resistance of the damaged through bolt to the ground and localization of damage to the bolt end-region, suggest that the insulation around the end-region was damaged, which resulted in a short circuit between the bolt and the core bar precisely at the point of insulation destruction (as shown in Fig. 2). This resulted in a large eddy current loss in the bolt and subjected it to a significant alternating electromagnetic force, thereby inducing a reciprocating vibration that eventually led to bolt overheating, melting, and fatigue fracture.

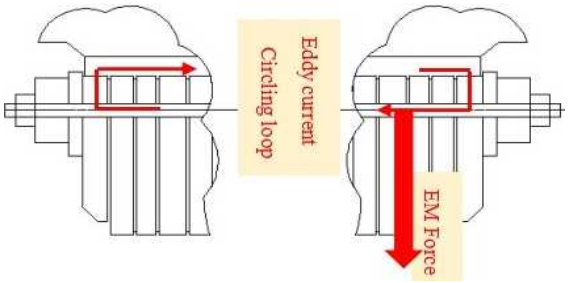

Fig. 2. Short circuit occurring between the through bolt and core bar, precisely where the bolt end insulation is destroyed

Table 1. Basic description of normal and failure conditions

	Description of the situation
Normal	bolt insulation is normal; no short circuit
Failure	bolt end insulation damage; short circuit occurs between the through bolt and core bar

Table 2. Basic generator data

Parameter	Value
Rated power (MW)	32.8
Rated voltage (kV)	10.5
Rated current (A)	1958
Power factor	0.92
Number of magnetic poles	44
Number of through bolts	132
Stator slot skewed degree	1slot
External diameter of stator (mm)	6020
Inner diameter of stator bore (mm)	5620
Stator core length	1400
Number of stator slots	264
Number of parallel branches of stator winding	1

To test these assumptions, the eddy current loss, electro-magnetic force, and natural frequency of a bolt under normal and fault conditions were calculated and compared using field-circuit coupling and modal analysis. The generator studied here has 132 through bolts on its stator; after running for 386 days, 21 bolts were damaged. The basic descriptions of the normal and failure conditions are listed in Table 1, with generator data listed in Table 2.

2.2 Boundary value problem for moving electro-magnetic field

A pole region that included the stator housing was chosen as the electromagnetic field calculation location. Considering the stator skew structure and its alignment along the z axis, the generator was divided into five slices, as shown in Fig. 3.

Assuming saturation of the iron core, the governing

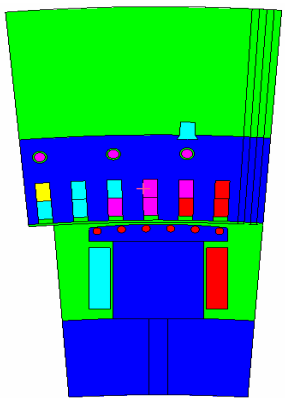

Fig. 3. Electromagnetic field problem region(multi-slice model of stator skewed structure, the generator was divided into five slices along the z axis)

equation of a nonlinear, time-varying electromagnetic moving field [19] can be used:

$$\nabla\times(\nu\nabla\times\mathbf{A})+\sigma\left[\frac{\partial\mathbf{A}}{\partial t}-\mathbf{V}\times(\nabla\times\mathbf{A})\right]=\mathbf{J_S} \tag{1}$$

where **A** is the vector magnetic potential, $\mathbf{J_s}$ is the source current density, ν is the reluctivity, **V** is the velocity, and σ is the conductivity.

In the multi-slice moving electromagnetic field model, the current density and vector magnetic potential of each slice are solely in the axial (z) direction, and the velocity is solely in the circumferential (x) direction. Assuming the Coulomb norm $\nabla\cdot\mathbf{A}=0$ and applying the boundary conditions of the problem region, the 2D boundary value problem of the nonlinear time-varying moving electromagnetic field for the generator is then obtained as

$$\begin{cases}\dfrac{\partial}{\partial x}(\nu\dfrac{\partial A_{slz}}{\partial x})+\dfrac{\partial}{\partial y}(\nu\dfrac{\partial A_{slz}}{\partial y})=-J_{slz}+\sigma\dfrac{\partial A_{slz}}{\partial t}+V_x\sigma\dfrac{\partial A_{slz}}{\partial x}\\ A_{slz}\big|_{arc\_in}=A_{slz}\big|_{arc\_out}=0\\ A_{slz}\big|_{ancyclic\_boundary\_start}=-A_{slz}\big|_{ancyclic\_boundary\_end}.\end{cases} \tag{2}$$

where V_x is the x-component of the velocity, J_{slz} is the axial z-component of the source current density, and A_{slz} is the axial z-component of the vector magnetic potential.

2.3 Coupling circuits

To determine the influence of important factors such as stator end winding, load condition of the generator, and short circuiting between the through bolt and core bar, a coupling circuit model was established (Fig. 4 and Fig. 5) and the resulting circuit equations was combined with the generator electromagnetic equations [8-15].

Based on the stator coupling circuit shown in Fig. 4, the voltage equation of stator circuit is

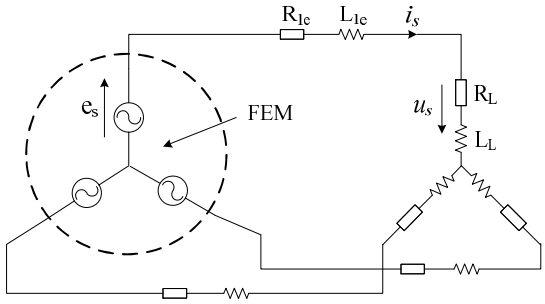

Fig. 4. Coupling circuit of the stator

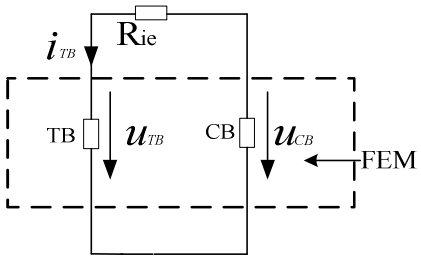

Fig. 5. Coupling circuit of the through bolt and core bar

$$e_s=u_s+R_{1e}i_s+L_{1e}\frac{di_S}{dt} \tag{3}$$

where e_s, u_s, and i_s are the inductive EMF, voltage, and current in the stator phase winding, respectively. The R_{1e} and L_{1e} are the resistance and leakage inductance of the stator end winding, respectively, provided by the generator manufacturer. R_L and L_L are the resistance and inductance of the load, respectively. The values of the latter two parameters can be changed to set different load operation conditions in the generator.

The circuit connecting the through bolt and core bar is shown in Fig. 5 and is represented by the following voltage equation:

$$U_{TB}-U_{CB}=i_{TB}R_{ie} \tag{4}$$

where the indices TB and CB represent the through bolt and core bar, respectively, which are both set as solid conductors in the circuit. U_{TB} and U_{CB} are the inductive voltages of the through bolt and core bar, respectively, i_{TB} is the current through the bolt and core bar, and R_{ie} is the resistance between the through bolt and core bar. When the through-bolt insulation is normal, R_{ie} is very large, but under a short circuit between the through bolt and core bar R_{ie} approaches zero.

Combining the above circuit and electromagnetic equations, the magnetic vector potential A_{slz} of the generator slices was calculated by using the time-step finite element (FE) method to obtain the eddy current loss and electromagnetic force of the bolts as follows.

For the j^{th} layer of the multi-slice model, the eddy current density of the k^{th} bolt is

$$J_{TB} = -\sigma_b \frac{\partial A_{slz}}{\partial t} + \sigma_b \frac{u_{TB}}{l_b} \tag{5}$$

where σ_b and l_b are the conductivity and length of the bolt, respectively.

The current and loss of each mesh of the bolt's j^{th} layer are

$$I_e = \iint_{\Delta_e} J_{TB} dxdy \tag{6}$$

$$p_e = I_e^2 \frac{l_{bsl}}{\sigma_b \Delta_e} \tag{7}$$

where l_{bsl} is the length of the j^{th} layer bolt, and Δ_e is the area of the related mesh of the bolt.

The eddy current loss of one bolt is

$$p_{TB} = \sum_{j=1}^{N_{cl}} \sum_{e=1}^{N} p_e \tag{8}$$

where N is the number of meshes of one bolt in each slice, and N_{cl} is the slice number of the model.

The electromagnetic force of the bolt can be obtained according to the following equation:

$$\mathbf{F} = \int_v \mathbf{J} \times \mathbf{B} dV \tag{9}$$

where J is the current density in the bolt, and B is the magnetic density in the area where the bolt is located.

In addition, the induced voltage of the bolt can also be obtained in conjunction with Eq. (4).

3. Electromagnetic Computation Results and Discussion

The parameters R_{ie}, R_L, and L_L from Table 3 were used to perform simulations of the normal and failure conditions. The resulting electromagnetic field distribution in the stator core, induced voltage and eddy current losses, and radial electromagnetic force on the through bolt under the normal and short circuit stabilization states are shown in Figs. 6 and 7 and listed in Table 4.

From the above results, the following conclusions can be drawn:

– When the through-bolt insulation is normal, its eddy current, loss and electromagnetic force are very small (almost negligible).

Table 3. Some calculation parameter settings

Condition	R_{ie} (Ω)	R_L (Ω)	L_L (H)
Normal	1×10^9 Ω	2.8483	0.0039
Failure	1×10^{-9} Ω	2.8483	0.0039

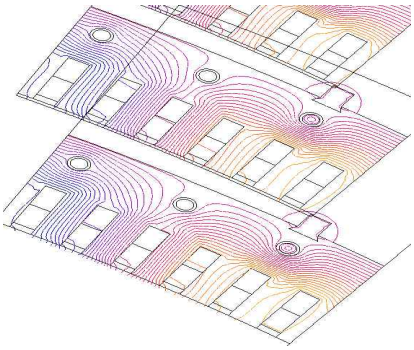

(a) Stator magnetic flux line

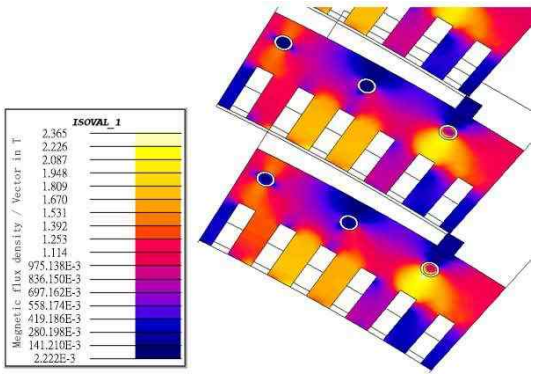

(b) Stator magnetic flux density

Fig. 6. Electromagnetic field distributions under the fault condition

Table 4. The comparison of the calculation results under the normal and fault conditions

Parameters	Values	
Insulation condition of bolt	Normal	Failure
Induced voltage of bolt /V(effective value)	12.37	2.64
Eddy current losses of bolt /W(average value)	0.58	2457.61
Eddy current loss density of bolt / W/m^3(average value)	1.19×10^3	5.07×10^6
Loss Density proportion to winding bar (average value)	1	18.55
Electromagnetic Force of bolt /N (peak-peak value)	0.24	2099.10

– When a short circuit occurs between a through bolt and core bar, the bolt incurs an average loss of up to 2-3 kW and a loss density greater than 5×10^6 W / m^3, which is 18 times the loss in the winding bar. We also determined that, because the bolt is inserted in the stator core, its cooling conditions are poor, particularly in the region near the short circuit locations of the bolt end. When the insulation of the bolt end-region incurs damage, the damaged location is filled with air; as the conductivity of air is only one-tenth that of the insulation, the cooling condition of this area becomes particularly bad, leaving the bolt end-region prone to overheating, melting, and breakdown. The thermal conductivities of air and the insulation material are listed in Table 5.

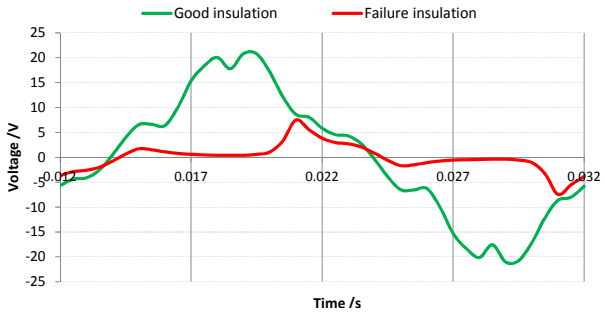

(a) Induced voltage

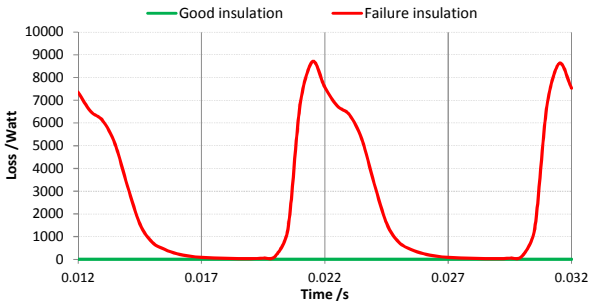

(b) Eddy current losses

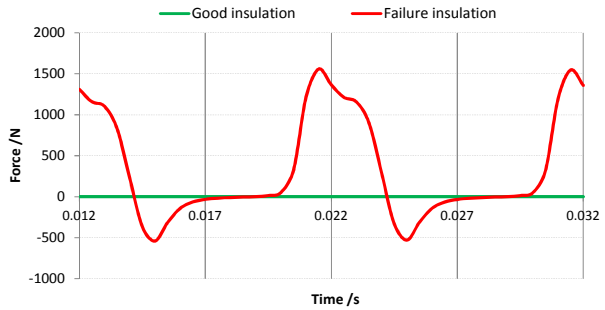

(c) Radial electromagnetic force

Fig. 7. Comparison of induced voltage, eddy current loss, and electromagnetic force on through bolt under fault and normal conditions

Table 5. Thermal conductivities of Insulation and air

Material	Thermal conductivity(w/m/K)
Insulation	0.22
Air	0.027

– Short circuiting between a through bolt and core bar also results in an added radial electromagnetic force with a frequency of 100 Hz (twice the power frequency) and a peak–peak value of more than 2,000 N. If the bolt is not sufficiently fixed, its natural frequency can change, with a strong resonance accompanied by additional bolt damage occurring if the natural frequency approaches 100 Hz.

4. Modal Analysis of Through Bolt

To study the influence of bolt fixation on the bolt's natural frequency, modal analysis of a bolt was carried out.

4.1 Influence of bolt assembly tensioning force on the natural frequency

According to design requirements, after a bolt is assembled its assembly tensioning force should be about 3.8 tN. However, long-term vibration and the hot–cold cycle in the stator core will cause the assembly tensioning force in the stator core to decrease gradually.

The modal analysis results listed in Table 6 show the influence of bolt assembly tensioning force on the natural frequency of bolt vibration.

Table 6. The influence of assembly tensioning force on the natural frequency

Condition	Natural frequency(Hz)			
	1st	2nd	3rd	4th
No tensioning force	34.0	97.2	185.1	306.5
With tensioning force	55.15	138. 21	224.99	351.32

From the table results, it can be seen that reducing the through-bolt assembly tensioning force from the design value to zero causes the second-order natural frequency to drop from 138 to 97.2 Hz. From the preceding electromagnetic force calculation results, 97.2 Hz is very close to the electromagnetic force frequency of the bolt under the failure condition (100 Hz), suggesting that a short circuit between the through bolt and core bar will result in strong bolt vibration.

4.2 Influence of bolt fixed point number on the natural frequency

To effectively forestall forced bolt vibration, we considered how the bolts might be fixed more strongly to the stator assembly. To carry out the analysis, the influence of the number of bolt fixed points on the bolt natural frequency was analyzed at an assembly tensioning force of zero. The results for two and seven fixed points are listed in Table 7 and shown in Figs. 8 and 9, respectively. The former scheme using two fixed points is found in the original faulty generator design, in which the fixture points are both located in the bolt end-region.

The results, as shown in the table and figures, indicate that increasing the number of fixed points from two to seven changes the natural frequency to effectively avoid forced vibration.

Table 7. Influence of bolt fixed number on the natural frequency

Fixed point number	Natural frequency(Hz)			
	1	2	3	4
2 (both located in bolt end)	34.0	97.2	185.1	306.5
7	983.5	986.3	993.5	1,001

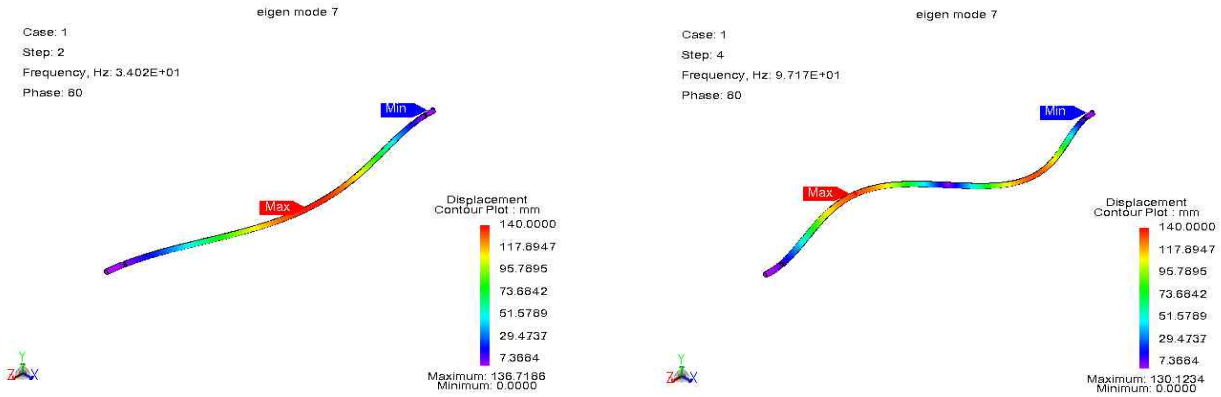

(a) First-order mode shape (b) Second-order mode shape

Fig. 8. Two fixed-points condition

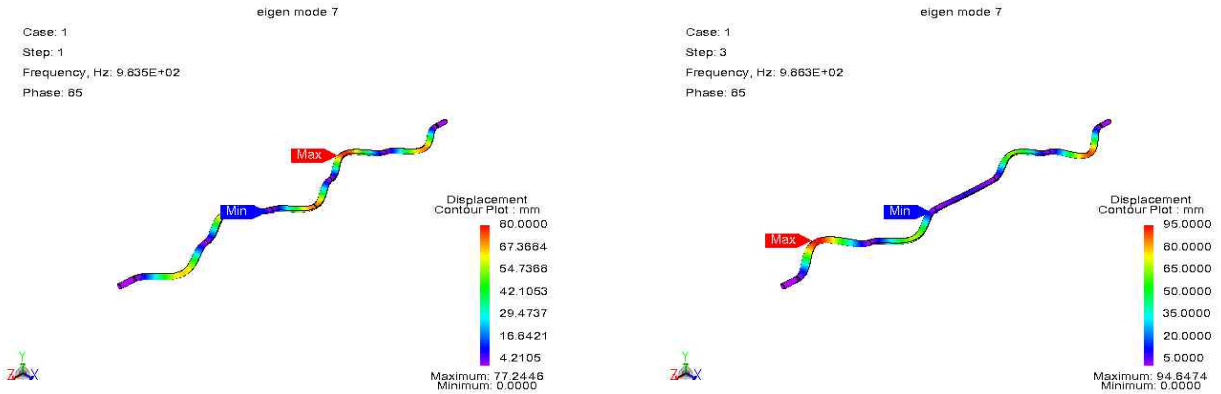

(a) First-order mode shape (b) Second-order mode shape

Fig. 9. Seven fixed-points condition

5. Failure Mechanism Summary and Improvement Design Measures

5.1 Failure mechanism summary

Based on the calculation results described in this paper, the through-bolt failure mechanism can be summarized as follows:

– Over a long duration of generator operation, the bolt assembly tensioning force decreases, reducing the natural frequency of the bolt vibration to around 100 Hz. At the same time, core self-excitation induces continuous vibration in the two-point fixed bolt, gradually destroying the insulation near the fixed points.

– If the greasy dirt buildup on the bolt end-region is not cleaned, the bolt end-region insulation situation further deteriorates.

– Once the insulation on the bolt end is damaged, a short circuit occurs between the through bolt and the core bar. This leads to bolt overheating and melting as well as to an alternating electromagnetic force with a peak-peak value greater than 2,000 N and a frequency of 100 Hz. These factors further aggravate vibration, damaging the bolt.

5.2 Goal for improvement design measures

In view of the failure mechanism described above, the following improvement measures were applied to the generator:

– A new insulation structure comprising three layers of impregnated glass cloth composite, insulating bushing, and silicone rubber self-adhesive tape was applied to the bolt assembly. This significantly improved bolt insulation performance and provided multi-fulcrum contact between the bolt and the stator core, effectively altering the natural frequency of the bolt assembly and reducing insulation damage from bolt vibration.

– As a prophylactic against insulation damage and short circuiting, a special insulation and anti-oil treatment program was applied to the assembly structure at the through bolt's upstream and downstream sides (backing ring, bushing, butterfly spring, etc.).

–The through-bolt material was improved by replacing the ordinary 35CrMo round steel with hardened and tempered 34CrNiMo round steel. This significantly improved the bolt tensile strength, yield point, and shearing strength.

6. Conclusion

The above improvement measures were adopted in the failed generator in March 2013, after which the generator operated for 36 months and a new maintenance regime was implemented in March 2016. During the overhaul, no failure was found.

The results of the improvement regime and successful overhaul demonstrate that the analysis in this study of the failure mechanism was accurate and reasonable and the improvement measures were correct and effective. Therefore, it can be concluded that the simulation model and results of this paper have been satisfactorily verified (indirectly).

The findings reported in this study will help to improve the quality of the design and manufacture of similar generator units and ensure their safe and stable operation.

In future work, we will try to convince some of China's generator manufacturers to allow us to reproduce such failures by destroying the bolt end insulation in the manufacturing company's workshop. We would then use the direct test method to further verify the simulation model and results of this paper, and write a new paper to conduct the relevant analysis and discussion.

Acknowledgment

This work was sponsored by the National natural sciences fund youth fund of China, No.51607146 and 61703345, and the Key Scientific Research fund project of Xihua University, No.Z1520907 and Z1520909, and the Key Research fund projects of Si chuan Provincial Education Department, No.16ZA0155 and 16ZB0159. And this work was supported by Sichuan Science and Technology Program, No.2018GZ0391, and this work was supported by a grant from Chunhui Project Foundation of the Education Department of China, No. Z2016144. Supported by Sichuan Provincial Department of Science and Technology (No. 2017JY0204), China. And it was sponsored by The Key Laboratory of Fluid and Power Machinery, Ministry of Education, Xihua university, Chengdu 610039, China, and the International cooperation project of Chengdu science and Technology Bureau,No. 2016-GH02-00111-HZ, and the Scientific and Technological Research Program of Chongqing Municipal Education Commission, No. KJ1713351.

References

[1] Knight, A.M., Karmaker, H., and Weeber, K., "Prediction of damper winding currents and force harmonic components in large synchronous machines," *Proc. 15th ICEM, Brugge*, *West Flanders, Belgium*, 2002, vol. 35.

[2] Knight, AM., Karmaker, H., and Weeber, K., "Use of a permeance model to predict force harmonic components and damper winding effects in salient pole synchronous machines," *IEEE Trans. on Energy Conversion*., 2002, vol. 17, no. 4, pp. 478-484.

[3] Traxler-Samek, G., Lugand, S., and Schwery, A.: "Add loss in the damper winding of large hydrogenerator at open-circuit and load conditions," IEEE Trans. on Industrial Electronics., 2010, vol. 57, no. 1, pp. 154-160.

[4] Keller, S., Xuan, M. T., Simond, J. J., and Chewry, A., "Large low-speed hydro-generator-unbalanced magnetic pulls and additional damper losses in eccentricity conditions," *IET Electr. Power Appl*., 2007, vol. 21, no. 5, pp. 657-664.

[5] Keller, S., Xuan, N.T., and Simond, J.J., "Computation of the no-load voltage waveform of laminated salient-pole synchronous generators," *IEEE Trans. on Industry Appl*., 2006, vol. 42, no. 3, pp. 681-687.

[6] Kim, C.E., and Skyulski, J.K., "Harmonic analysis of output voltage in synchronous generator using finite element method taking account of the movement," *IEEE Trans on Magnetics*., 2002, vol. 38, no. 2, pp. 1249-1252.

[7] SWang, S., Wang, X., Wang, Y., Li, P., Su, W., Ma, and Zhang, G., "Steady-state performance of synchronous generators with ac and dc stator connections considering saturation," *IEEE Trans. on Energy Conversion*., 2002, vol. 17, no. 2, pp. 176-182.

[8] Piriou, F., and Razek, A., "Finite element analysis in electromagnetic systems accounting for electric circuits," *IEEE Trans on Magnetics*., 1993, vol. 29, no. 2, pp. 1669-1675.

[9] Sarikhani, A., Nejadpak, A., and Mohammed, O.A., "Coupled field-circuit estimation of operational inductance in PM synchronous machines by a real-time physics-based inductance observer," *IEEE Trans. on Magnetics*., 2013, 49, (5), pp. 2283-2286.

[10] Huangfu, Y., Wang, S., Qiu, J.,Zhang, H., Wang, G., and Zhu, J., "Transient performance analysis of induction motor using field-circuit coupled finite-element method," *IEEE Trans. on Magnetics*., 2014, 50, (2), pp. 2283-2286.

[11] Weilharter, B., Biro, O., Rainer, S., Stermecki, A.: 'Computation of rotating force waves in skewed induction machines using multi-slice models," *IEEE Trans on Magnetics*, 2011, vol. 47, no. 5, pp. 1046-1049.

[12] Keranen, J., Ponomarev, P., Pippuri, J., et al.: 'Parallel performance of multi-slice finite-element modeling of skewed electrical machines," *IEEE Trans on Magnetics*, 2017, vol. 53, no. 6, pp. 1204-1207.

[13] Fan, Z., Liao, Y., Han, L., and Xie, L.D., "No-load voltage waveform optimization and damper bars heat reduction of tubular hydro-generator by different degree of adjusting damper bar pitch and skewing

stator slot," *IEEE Trans. on Energy Conversion*., 2013, vol. 28, no. 3, pp. 461-469.
[14] Zhen-nan, F., Li-Han, Yong, L., Li-dan, X., Kun, W., Jun, W., Xiu-cheng, D., and Bing, Y., "Effect of damper winding and stator slot skewing structure on no-load voltage waveform distortion and damper bar heat in large tubular hydro generator," *IEEE Access*, 2018, vol. 6, no. 1, pp. 22281-22291.
[15] Baojun, G.E., Mingzhe, L., Yutian, S.U.N., Jinxiang, L., and Lijie, H.U., 'Calculation of damper winding current for synchronous generators under asymmetric conditions," *Proc. CSEE*., 2013, vol. 33, no. 27, pp. 153-161.
[16] Xia, H., Yao, Y., and Ni, G., "Analysis of ventilation fluid field and rotor temperature field of a generator," *Electric Machines and Control*., 2007, vol. 11, no. 5, pp. 472-476.
[17] Weili, L., Zhang, Y., and Yonghong, C., "Calculation and analysis of heat transfer coefficients and temperature fields of air-cooled large hydro-generator rotor excitation windings," *IEEE Trans. on Energy Conversion*., 2011, vol. 26, no. 3, pp. 946-952.
[18] Weili, L., Chunwei, G., and Yuhong, C., "Influence of rotation on rotor fluid and temperature distribution in a large air-cooled hydrogenerator [J]," *IEEE Trans On Energy Conversion*., 2012, vol. 28, no. 1, pp. 117-124.
[19] Hu, M.Q., and Huang, X.L., "Numerical computation method and its application of electric machine performance," (Southeast University Press, 2003, pp. 16-30).

Zhi-ting Zhou She was born in Deyang, China in 1999. She is currently pursuing the B.Eng. degree at Xihua University. Her research interests include magnetic and thermal field calculation of generators, electrical machinery, and motor drives.

Zhen-nan Fan He was born in Longchang, China in 1981. He received his Ph.D. degree in electrical engineering from Chongqing University, Chongqing, China, in 2013. He is currently an associate professor at Xihua University. His research interests include magnetic and thermal field calculation of generators, electrical machinery, and motor drives.

Jian-fu Li He received the M.Sc. degree from Huazhong University of Science and Technology University, Wuhan, China, in 2007. He is currently a senior engineer at Dong Fang Electrical Machinery Co., Ltd. His research interests include magnetic and thermal field calculation of generators, electrical machinery, and motor drives.

Kun Wen He was born in Chongqing, China in 1991. He is currently pursuing the M.Sc. degree at Xihua University. His research interests include magnetic and thermal field calculation of generators, electrical machinery, and motor drives.

Bi-de Zhang He born in 1975,received his doctor's degree from Chong University in 2002.He is employed in xihua university as a professor in the field of electrical engineering. His research interest is on-line monitoring and fault diagnosis of electrical equipment.

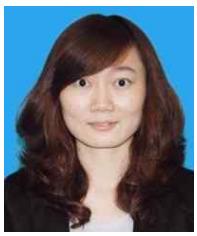

Tao Wang She was born in Chengdu, China, in 1986. She received the Ph.D. degree in electrical engineering from Southwest Jiaotong University, Chengdu, China, in 2016. She is currently a lecturer at Xihua University. Her research interests include magnetic and thermal field calculation of generators, electrical machinery, and motor drives.

Yan-kun Xia He was born in Huanggang, China in 1984. He received the Ph.D. degree in electrical engineering from Southwest Jiaotong University, Chengdu, China, in 2014. He is currently a lecturer at Xihua University. His research interests include magnetic and thermal field calculation of generators, electrical machinery, and motor drives.

Zhang Sun He was born in Lichuan, China in 1986. He received his M.Sc. degree from Xihua University, Chengdu, China, in 2013. Currently, he is a lecturer at Xihua University. His research interests include magnetic and thermal field calculation of generators, electrical machinery, and motor drives.

Bing Yao He was born in Sichuan, China in 1981. He received the M.Sc. degree Xihua University, Chengdu, China, in 2010. He is currently a lecturer at Xihua University. His research interests include magnetic and thermal field calculation of generators, electrical machinery, and motor drives.